



Manufacturing Science and Education 2025

ACTA TECHNICA NAPOCENSIS

Series: Applied Mathematics, Mechanics, and Engineering

Vol. 68, Issue Special II, Month July, 2025

## INFLUENCE OF INFILL DENSITY ON COMPRESSIVE PERFORMANCES OF PEI 1010 PARTS MANUFACTURED BY FUSED FILAMENT FABRICATION PROCESS

**Radu TORPAN, Sebastian - Marian ZAHARIA, Lucia – Antoneta CHICOS,  
Mihai Alin POP, Camil LANCEA**

**Abstract:** *This study investigates the properties of 3D printed Polyetherimide 1010 (PEI 1010), focusing on the influence of infill density on mechanical performance. Compressive tests were conducted to evaluate the material's strength and stress – strain behavior at varying infill levels. Additionally, microscopical analysis and hardness tests were conducted in order to characterize the Fused Filament Fabrication (FFF) process for PEI 1010. Results demonstrate that infill density significantly enhances the mechanical properties of PEI 1010, making it a viable option for applications requiring high-performance materials.*

**Keywords:** *3D printing, PEI 1010, infill density, compressive tests, microscopical analysis, hardness.*

### 1. INTRODUCTION

One of the most widespread additive manufacturing processes is represented by the fused filament manufacturing process also called FFF (Fused Filament Fabrication). It consists in heating a filament to the point of flow (glass transition) in which the molten material cools quickly, in contact with the external environment and solidifies, thus resulting in a model in layers, obtaining the finished product [1]. The main materials used in the FFF process include PLA (polylactic acid), PC (polycarbonate), ABS (acrylonitrile butadiene styrene), but also high-strength polymers such as PEEK (polyether ether ketone) or PEI/ULTEM (Polyetherimide) [2]. The versatility of the FFF process comes from the variation in fabrication parameters. The variation of wall thickness and number of walls [3, 4], printing speed and printing temperature [5], as well as infill density and internal geometry have a major impact on the mechanical strength of 3D printed parts [6, 7]. Using various printing strategies [8] in the choice of infill geometry (rectilinear, grid or honeycomb), but also the variation of the degree of filling, results in parts with anisotropic behavior, which do not have the same properties

along the three 3D printing directions that define the printed part [9].

One of the most important parameters of the parts, made through the FFF process, is represented by the infill density. This parameter plays an important role because it greatly influences the mechanical resistance of the parts, thus a causal relationship can be determined between the increase in the percentage of infill density and the mechanical resistance [10]. In order to obtain superior mechanical performance of the PEI/ULTEM parts subjected to compression stress, made by the FFF process, it is necessary to control the process parameters, such as the ambient temperature in which the 3D printing is carried out because the temperature of the lower layer over which the successor layer is deposited directly influences the mechanical properties of the final product. Thus, as the ambient temperature increases, the cohesion between the layers increases, resulting in enhanced mechanical characteristics [11]. The compressive strength is also influenced by the pattern adopted for the infill density. Among the most common internal configurations for the infill density pattern (grid, triangle, honeycomb, gyroid and cubic) for parts that are mainly subjected to uniaxial compressive stresses, the

best results were obtained using the grid pattern [5], but for parts with compound stresses on several axes, the cubic pattern has superior results, especially for parts made of high-strength polymers such as PEEK. [12].

Although, when parts are printed using the FFF process, with the ULTEM 9085 filament, a variation of the results is found for tensile analysis, for parts that are printed in different directions (X,Y and Z) [13], these shortcomings can be mitigated as shown in a recent study [14] on parts of ULTEM 1010 by local laser heat treatment of the area to be printed to improve adhesion between the layers, which causes a significant increase in the mechanical strength of the parts. In another study [15] the impact on mechanical strength and hardness was analyzed by annealing parts made of PEI/ULTEM 1010 by the FFF process, highlighting that the optimal temperature for annealing is 225 °C. The annealing process improves the bonds between the layers and the mechanical properties of the material, solving crystallinity problems caused by rapid cooling. Thus, the tensile strength for the non-heat-treated parts was 68 MPa, and the tensile strength for the annealed parts at the temperature of 225 °C was 75 MPa, which causes a 10% increase in tensile strength. In contrast, the same study [15] finds an increase in hardness (Shore D) directly proportional to the increase in annealing temperature, starting from 72 units (Shore D) for non-heat-treated parts and reaching a hardness of 81 units (Shore D) for specimens treated at 235 °C. The results confirm the effectiveness of annealing at various temperatures for 180 min to improve the performance of PEI 1010 filament [15].

However, from the current state of research it can be seen that for the PEI 1010 material there is no specific information on the compression behavior. The present paper deals with the variation of infill density in relation to the compression performance (stress-strain curves, compression strength and compression modulus) that is performed on the 3D printed specimens and analyzes their microscopic appearance before and after testing. Also, in this study, the samples manufactured by the FFF process from the PEI 1010 filament were analyzed microscopically and from the point of view of hardness.

## 2. MATERIALS AND METHODS

In this study, specimens made by the FFF process of the KIMYA PEI 1010 material with various filling percentages were subjected to compression tests and microscopic analysis to determine the relationship between infill density and compressive strength. Also, the parts made of PEI 1010 material, manufactured in a closed environment and at a controlled temperature (see Table 2), were analyzed microscopically. The mechanical properties of the parts made with PEI 1010 filament are included in Table 1, as indicated by the manufacturer [16].

*Table 1*

**Mechanical properties of the material KIMIA PEI 1010 [16].**

Property	Standard	Value	Unit
Tensile modulus	ISO 527	2917.5	MPa
Tensile Strength	ISO 527-2/1A/50	90.9	MPa
Tensile strain at strength	ISO 527-2/1A/50	5.6%	N/A
Tensile Stress at Break	ISO 527-2/1A/50	90.9	MPa
Flexural modulus	ISO 178	2236	MPa
Deformation at Flexural Strain	ISO 178	>5%	N/A
Shore Hardness	ISO 868	84.5	N/A

Geometry of the specimens was three-dimensionally modeled (Figure 1), in accordance with the ASTM D695-15 standard [17]. This standard applies to the determination of the mechanical properties of plastics, including composite materials, when subjected to compression at uniform and relatively low velocities. The specimens have a cylindrical shape, with a diameter of 12.7 mm and a height of 25.4 mm [17]. Next step consists in preparing the specimens for fabrication using the Simplify3D 5.1.1 software system, where the fabrication parameters of each set of specimens were defined. Specimens subjected to compression testing were 3D printed with the MiniFactory Ultra digital 3D printing system using the process parameters contained in Table 2. For a more detailed determination of the compression behavior as a function of the infill density variation of the PEI 1010 material, a test increment of 15% was chosen. The result was 7

sets, of 5 specimens each, printed at an infill density of 15%, 30%, 45%, 60%, 70% and 90% (Figure 2). To have a complete picture of the results, a set of 5 specimens was also printed at 100% infill density.

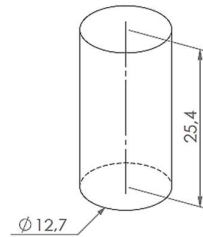


**Fig. 1.** CAD geometry of the specimens subjected to compression (dimensions in mm).

**Table 2**  
*Manufacturing parameters of the FFF process for PEI 1010 filament compression tested specimens.*

FFF parameters	Value
Layer height	0.25 mm
Top/ Bottom solid layers	5
Outline perimeters	3
Infill density	15%, 30%, 45%, 60%, 75%, 90%, 100%
Internal infill pattern	Grid
Extrusion temperature	385°C
Heated bed	220°C
Heated chamber	215°C
Printing speed	35 mm/sec

The chosen infill pattern is the grid type (Figure 2), as it has the highest consistency inside the 3D printed specimens, presenting a constant number of vertical and horizontal linear structures, for the specimens within the same set of filling density.

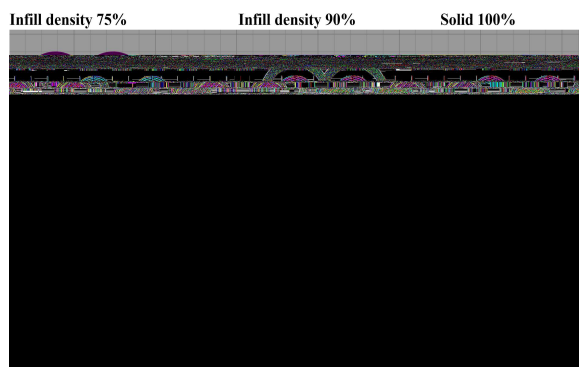


**Fig. 2.** Infill density variation on the 7 sets of specimens.

The compression tests were performed on the WDW 150 S equipment, with a test speed of 10 mm/min. The microscopic analysis of the layers of extruded material was carried out on the Leica Emspira 3 optical microscope. Previously, one tested and one untested specimen were embedded in epoxy resin and sectioned longitudinally to assess the cohesion between the layers and possible defects in the adhesion of the successive layers (bonding the upper and lower layers), and transversely to assess the internal structure of the specimen. The samples were sanded with 600, 1200, 1500, 2000 and 2500 grit sandpaper using the Buehler Phoenix Beta Grinder.

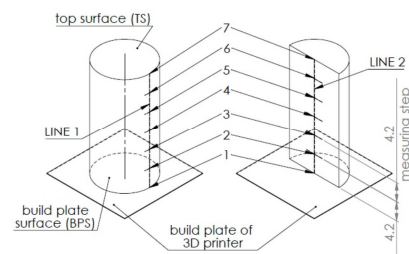


**Fig. 3.** Identification of the areas where the hardness measurement was performed on the untested specimen (dimensions in mm)

For the Shore D hardness analysis, untested specimens with the grid filling pattern and 100% infill density were analyzed. 7 measurements of the hardness on the surface of the first printed layer (BPS), of the last printed layer (TS), on the outer surface of the cylinder on its generator (LINE 1) and inside the part on the axis of revolution (LINE 2) are revealed. The measurements made along the two lines of interest start from the first printed layer, continue with a step of 4.2 mm, and the last determination being made on the last 3D printed layer. In the case of measurements on circular surfaces, they are carried out at equidistant intervals and uniformly distributed on the surface of the part.

### 3. RESULTS AND DISCUSSIONS

#### 3.1 Compression test results

The compression testing of the 3D printed parts from PEI 1010 has the main purpose of evaluating the compression strength, the modulus of elasticity under compression and the

stress-strain curves (Figure 4). The stress-strain curves (Figure 4) shows that an important compression characteristic of the PEI 1010 material, namely that it presents a high rigidity, this aspect being in accordance with the manufacturer's specifications [16]. This stiffness, together with the defects specific to 3D printing, determines a random character in terms of strain for the PEI 1010 material. Also, the specimens with lower infill density (15%, 30% and 45%) can accumulate more energy before failure and therefore show a strain close to the parts with higher infill density (60%, 75%, 90% and 100%). It can be stated that in the case of PEI 1010 parts, the increased stiffness and exceptional dimensional stability [16] determined a different strain response depending on the filling density.

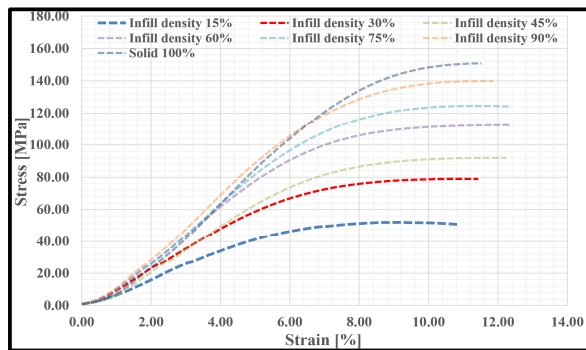


**Fig. 4.** Stress-strain curves for compression of 3D printed parts from PEI 1010.

Increasing the infill density of 3D printed parts causes an increase in their compressive strength, as can be seen in Figure 5. However, the relationship between compressive strength and filling density is not always linear and perfectly proportional, as it depends on many factors

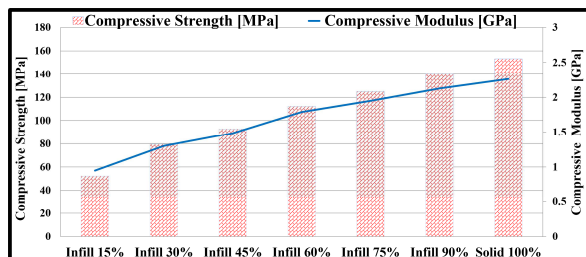


**Fig. 5.** Average values of compression results.

. Thus, it is found that the specimens with 100% filling density have the highest

compressive strength (153 MPa), and the specimens with the lowest compressive strength (52 MPa) are obtained at 15% filling density.

### 3.2 Results of microscopic analyses

After performing the compression tests, the 3D printed parts suffered a local buckling associated with the barrel effect, specific to this type of stress. Microscopic analysis revealed a brittle fracture crack (Figure 6), which appears suddenly in materials with high stiffness, without significant plastic deformation. Also, in Figure 6, you can see the classic defects (triangular and diamond voids) appearing in the FFF process. In Figure 7, it can be observed a microscopic image of the top surface (TS), where is highlighted the perimeter wall lines, and how the fill of the 100% infill specimens were 3D printed.

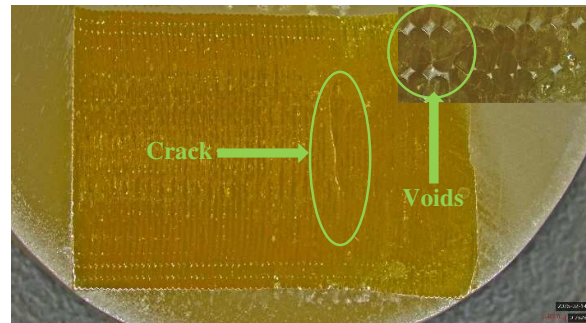


**Fig. 6.** Cross section of 3D printed parts with 100% infill density



**Fig. 7.** Top surface (TS) of 3D printed parts.

### 3.3 Results of the hardness analysis of the specimens

From the surfaces and lines of interest (Figure 3), with the help of the Shore D durometer, the hardness of the layers was revealed, and the results were centralized in Table 3. The mean hardness along line 1 was 82.42 Shore D units, while on line 2 the average hardness value is 88

units. At the BPS surface level the average hardness was 86.9 units, while at the top surface (TS) level the average hardness is 85.3.

Table 3

Data obtained from the Shore D measurement of the specimen with 100% infill density

Point of measurement	Geometry measured			
	LINE 1	LINE 2	BPS	TS
1	82	86	89	84
2	81	88	86	86
3	81	89	87	87
4	81	89	88	86
5	82	89	88	86
6	84	89	82	86
7	86	86	88	82
Average	82.4	88	86.9	85.3

The differences in hardness between the BPS and the TS are due to maintaining constant temperatures for a longer period of time during the additive manufacturing process, these results also being obtained in the study [15], which identified the fact that an increase in temperature causes an increase in hardness.

#### 4. CONCLUSIONS

In conclusion, the PEI 1010 material from the manufacturer KIMYA has increased rigidity but also specialized manufacturing conditions (printing temperatures and heated enclosure) to obtain consistent results. There is a direct causal relationship, although non-linear, between infill density and compressive strength. Thus, for the specimens printed with an infill density of 15%, the maximum compressive stress is 52 MPa, while for the specimens printed with an infill density of 100%, the maximum stress is 153 MPa. The stiffness of the groups the stress-strain curves in 2 categories, specimens manufactured with 15%, 30% and 45% infill and the rest of the specimens (60%, 75%, 90% and 100%). This phenomenon can be attributed to a higher energy absorption for the lower infill density group.

The average hardness of the manufactured parts is 85.65 Shore D units, although this varies between the lower surface 86.9 and the upper 85.3 surface. A phenomenon that reveals the importance of uniform heating during printing. The microscopic analysis of the tested

specimens reveals the classic manufacturing defects through the FFF process, triangular or diamond-shaped air voids, but also the mode of yielding to compression through the appearance of the barrel shape and the developed transverse crack. The material discussed in this study can have structural applications in the construction of aircraft (e.g. fairings, brackets or sliding bearings) but also in automotive domain, especially in areas that require good mechanical strength but also increased thermal resistance.

#### 5. REFERENCES

- [1] Liu, J., Naeem, M.A., Al Kouzbary, M., Al Kouzbary, H., Shasmin, H.N., Arifin, N., Abd Razak, N.A., Abu Osman, N.A. *Effect of Infill Parameters on the Compressive Strength of 3D-Printed Nylon-Based Material*, Polymers, ISSN: 2073-4360, 2023
- [2] Vázquez-Silva, E., Pintado-Pintado, J.A., Moncayo-Matute, F.P., Torres-Jara, P.B., Moya-Loaiza, D.P. *Effect of Infill Density on the Mechanical Properties of Natural Peek Processed by Additive Manufacturing*, Polymers, ISSN: 2073-4360, 2025
- [3] Wu, W., Geng, P., Li, G., Zhao, D., Zhang, H., Zhao, J., *Influence of Layer Thickness and Raster Angle on the Mechanical Properties of 3D-Printed PEEK and a Comparative Mechanical Study between PEEK and ABS*, Materials, ISSN:5834–5846, 2015
- [4] Wächter, J., Elsner, M., Moritzer, E., *Investigation of the Processability of Different PEEK Materials in the FDM Process with Regard to the Weld Seam Strength*, University of Texas at Austin, Austin, TX, USA, 2019
- [5] Bakhtiari, H., Nikzad, M., Tolouei-Rad, M., *Influence of Three-Dimensional Printing Parameters on Compressive Properties and Surface Smoothness of Polylactic Acid Specimens*, Polymers, ISSN: 2073-4360 2023
- [6] Yadav, P., Sahai, A., & Sharma, R. S., *Strength and Surface Characteristics of FDM-Based 3D Printed PLA Parts for Multiple Infill Design Patterns*, Journal of The Institution of Engineers (India): Series C, ISSN: 2250-2157, 2021
- [7] Rahman, K.M., Letcher, T., Reese, R. *Mechanical Properties of Additively Manufactured PEEK Components Using Fused Filament Fabrication*, ASME International Mechanical Engineering Congress and Exposition, Houston, TX, USA, 13–19 November 2015, American Society of

- Mechanical Engineers, New York, NY, USA, 2015
- [8] Sood, A.K., Ohdar, R.K., Mahapatra, S.S., *Experimental investigation and empirical modelling of FDM process for compressive strength improvement*, Journal of Advanced Research, ISSN: 2090-1232, 2012
- [9] Motaparti, K. P., Taylor, G., Leu, M. C., Chandrashekhara, K., Castle, J., Matlack, M., *Effects of Build Parameters on Compression Properties for Ultem 9085 Parts by Fused Deposition Modeling*, Proceedings of the 27th Annual International Solid Freeform Fabrication Symposium (2016, Austin), pp. 964-977, University of Texas at Austin, 2016
- [10] Abbas, T., Othman, F.M., Ali, H.B., *Effect of Infill Parameter on Compression Property in FDM Process*, International Journal of Engineering Research and Applications, ISSN: 2248-9622, 2017
- [11] Forés-Garriga, A., Pérez, M. A., Gómez-Gras, G., & Reyes-Pozo, G., *Role of infill parameters on the mechanical performance and weight reduction of PEI Ultem processed by FFF*, Materials and Design, ISSN: 0264-1275, 2020
- [12] Abbas, K., Hedwig, L., Balc, N., Bremen, S., *Advanced FFF of PEEK: Infill Strategies and Material Characteristics for Rapid Tooling*, Polymers, ISSN: 2073-4360, 2023
- [13] Vindedze, E., Glaskova-Kuzmina, T., Dejus, D., Jatnieks, J., Sevcik, S., Bute, I., Sevcenko, J., Stankevich, S., Gaidukovs, S., *Effects of Printing Orientation on the Tensile, Thermophysical, Smoke Density, and Toxicity Properties of UltemR 9085*, Polymers, ISSN: 2073-4360, 2025
- [14] Han, P., Tofangchi, A., Deshpande, A., Zhang, S., & Hsu, K., *An approach to improve interface healing in FFF-3D printed Ultem 1010 using laser pre-deposition heating*, Procedia Manufacturing, ISSN: 2351-9789, 2019
- [15] Yilmaz, M., Yilmaz, N. F., & Kalkan, M. F., *Rheology, Crystallinity, and Mechanical Investigation of Interlayer Adhesion Strength by Thermal Annealing of Polyetherimide (PEI/ULTEM 1010) Parts Produced by 3D Printing*, Journal of Materials Engineering and Performance, ISSN: 1059-9495, 2022
- [16] KIMYA PEI 1010 3D Filament, <https://www.crea3d.com/en/kimya/1244-2238-kimya-pei-1010-ultem.html>
- [17] ASTM D695, Standard Test Method for Compressive Properties of Rigid Plastics, ASTM Materials Standards, ASTM International: West Conshohocken, PA, USA, 2002

### **Influența densității de umplere asupra performanțelor la compresiune a pieselor din PEI 1010 fabricate prin procedeul de fabricare a filamentului fuzionat**

Acest studiu investighează proprietățile polieterimidei 1010 imprimate 3D (PEI 1010), concentrându-se pe influența densității de umplere asupra performanței mecanice. Au fost efectuate teste de compresiune pentru a evalua rezistența materialului și comportamentul la efort – deformare la diferite niveluri de umplere. În plus, au fost efectuate analize microscopice și teste de duritate pentru a caracteriza procesul de fabricare a filamentului fuzionat (FFF) pentru PEI 1010. Rezultatele au demonstrat că densitatea de umplere îmbunătățește semnificativ proprietățile mecanice ale PEI 1010, făcându-l o opțiune viabilă pentru aplicațiile care necesită materiale de înaltă performanță.

**Radu TORPAN**, PhD Student, Eng., Transilvania University of Brașov, Department of Manufacturing engineering, B-dul Eroilor No.29, Brașov, Romania, radu.torpan@unitbv.ro

**Sebastian-Marian ZAHARIA**, PhD Professor, Transilvania University of Brașov, Department of Manufacturing engineering, B-dul Eroilor No.29, Brașov, Romania, zaharia\_sebastian@unitbv.ro

**Lucia-Antoneta CHICOS**, Associate Professor, Transilvania University of Brașov, Department of Manufacturing engineering, B-dul Eroilor No.29, Brașov, Romania, l.chicos@unitbv.ro

**Mihai Alin POP**, Researcher II, Transilvania University of Brașov, Materials Science Department, B-dul Eroilor No.29, Brașov, Romania, mihai.pop@unitbv.ro

**Camil LANCEA**, PhD Professor, Transilvania University of Brașov, Department of Manufacturing engineering, B-dul Eroilor No.29, Brașov, Romania, camil@unitbv.ro